University of Thi-Qar Journal of Science (UTJsci)
E-ISSN: 2709-0256, P-ISSN: 1991-8690, Vol. 11, No. 1, Jun. 2024

Superparamagnetism Phenomenon for a Mixed Spin Ferrimagnetic Binary System

Aqeel Raad Ghafel*[1a] and Hadey K. Mohamad[1b]

[1] *Physics Department, College of Science, Al Muthanna University, Samawah, Iraq.*
[b]hadey.mohamad@mu.edu.iq,
[a*] Corresponding author: sci.akeel@mu.edu.iq.

Received: 2024-02-17, Revised: 2024-03-05, Accepted: 2024-03-08, Published: 2024-06-01

***Abstract*— A decorated ferrimagnetic mixed triangular system was studied using the molecular mean-field approximation. The outcomes of the investigation were examined using the Blume-Capel Ising model. The study paper investigates the influence of crystal and external magnetic fields on ferrimagnetic devices decorated with mixed spin-2 and spin-7/2 of a triangular lattice. It is noteworthy that spin-2 ions are located at the nodal points, whereas six additional spin-7/2 ions surround the proposed lattice. Altering the exchange interactions through the specific crystal and external magnetic fields induces superparamagnetic behaviours. New characteristics reveal that mixed spin triangular decorated ferrimagnets exhibit superparamagnetic behaviour at $D_A/|J_2|=-2.5$, with $J_1 = -0.5$ and $J_2 = -1.0$ in the range ($15 \leqslant K_BT/|J_2| \leqslant 18$). It is important to note that the total magnetization changes with the external magnetic field and affects the superparamagnetism phenomenon of a decorated mixed spin ferrimagnet when $D_A/|J_2| = 8$, and $D_B/|J_2|=-11$, $J_1 = -0.5$ and $J_2 = 1$, for $K_BT/|J_2| = 2, 2.5, 3, 3.5$, and 4 K° respectively.**

***Keywords*—Decorated ferrimagnets, triangular lattice, Nodal and decorating anisotropies, superparamagnetic behaviour.**

I. Introduction

Recently, ferrimagnetic materials have been the most magnetically important materials in various applications. The Ising model with mixed magnetic spins has become increasingly significant in recent years. The Ising models and their modifications have been widely regarded as crucial topics in statistical mechanics. They are characterized by the magnetization's instability caused by thermal agitation, leading to superparamagnetism [1,2]. Researchers have investigated these models' magnetic properties using methods such as mean-field theory, practical field theory, Monte Carlo simulation, etc. [3 V. Stubna and M. Jascur [4] used a generalized decoration iteration transformation to investigate a mixed spin-1/2 and spin-3/2 Ising model on a decorated square lattice the ground state and finite temperature phase boundaries are determined by finding a phases that correspond to the system's minimal internal or free energy. The researchers employed the mean-field approximation method to analyze the properties. M. Kerouac and Boughrara [5] Monte Carlo simulations examined the critical behavior and magnetic properties of a decorated Ising film on a cubic lattice framework. The system recognized double reentrants and one or two compensating points. R. Masrur et al. [6]. Conducted Monte Carlo simulations to model the magnetic characteristics of Ising spins with values of 5/2 and 3/2 on square and triangular lattices with additional decorations. The researchers determined the critical temperature at which the two-dimensional square and triangular lattices transformed. The authors investigated magnetization using exchange connections and crystal fields. Two-dimensional decorated square and triangle lattices monitored saturation magnetization and magnetic coercive field. M. Karmoua and N. De La Espriella [7] investigated a square lattice ferrimagnetic Ising system's critical point, first-order phase transition, and spin compensation behaviour. The system consisted of alternating spins of S-3/2 and S-5/2. The study employed Monte Carlo simulations and mean field theory. A twofold first-order phase transition was found to be temperature-dependent. Hadey K. Mohamad [8] used mean field theory to study a two-sublattice-adorned Blume Capel and found remarkable long-range order behaviour by altering magnetocrystalline anisotropies at both sites. Using a straightforward hydrothermal method, they manufactured superparamagnetic nanocomposites of MoS_2 nanosheets coated with magnetic Fe_3O_4 nanoparticles [10]. A. Jabar and R. Masrour [9] studied the phase diagrams of Ising models with spin-5/2 and spin-2 on a decorated square lattice. The study's main aim was to assess the magnetic characteristics of the ground state. The authors emphasized the significance of superparamagnetic systems. This research will study a Blume-Capel Ising model with mixed-spin ferrimagnetic properties using a developed mean field approximation (MMFA). We analyze the decorated triangular lattice containing N atoms. The lattices represent a mixed magnetic system comprising two sublattices, A and B, with magnetic spins $S_A = 2$ and $S_B = 7/2$, respectively. The analysis of the occurrence of superparamagnetism in the proposed system is illustrated in Fig.1. We investigate the correlation between the total magnetisation and the atoms' external and crystal magnetic fields to achieve this. The work is organized as follows: in section 2, we offer the basic framework of the relevant theory, giving the Hamiltonian operator of a decorated triangular lattice. In Section 3, we present the results and discussions. Finally, the conclusion is presented in Section 4.

This work is licensed under a Creative Commons Attribution 4.0 International License.
https://doi.org/10.32792/utq/utjsci/v11i1.1170

II. FORMALISM

The proposed ferrimagnetic system consists of a decorated triangular lattice consisting of a mixture of two sublattices, A and B, with spin values of (2,7/2). As depicted in Fig. (1), the Hamiltonian expresses the interactions between nearest neighbours, an external magnetic field, and the crystal field in the two-dimensional decorated triangular lattice.

$$\mathcal{H} = -J_1 \sum_{i,j} S_i^A S_j^B - J_2 \sum_{i,j} S_j^B S_j^B - D_A \sum_i \left(S_i^A\right)^2 - D_B \sum_j \left(S_j^B\right)^2 - H\left(\sum_i S_i^A + \sum_j S_j^B\right). \qquad (1)$$

Where $\mathcal{H}$ is a Hamiltonian measured by a Joule unit. J_1 is the nearest neighbour exchange parameter between magnetic atoms across the nodal and decorating ones. J_2 is the exchange interaction of the decorating atoms. And are the spins of atoms at sites i and j, respectively. D_A and D_B are single-ion anisotropies on A and B sites in Joule. Whereas H is the magnetic field in (Amp/m) unit. Spin S_i inhabited sublattice A with values of (±2, ±1,0), while S_j occupied the sublattice in the spin, which have the values of (±7/2, ± 5/2, ±3/2, ±1/2) are present in both networks.

The Hamiltonian expresses Blume-Capel Ising decorated lattices in the absence of an external magnetic field [11],

$$\mathcal{H} = -J_1 \sum_{i,j} S_i^A S_j^B - J_2 \sum_{i,j} S_j^B S_j^B - D_A \sum_i (S_i^A)^2 - D_B \sum_j \left(S_j^B\right)^2. \qquad (2)$$

So, one obtains

$$\mathcal{H}_A = -J_1 \sum_{i,j} S_i^A S_j^B - D_A \sum_i (S_i^A)^2. \qquad (3)$$

Using the Maxwell-Boltzmann distribution.

$$m_A = \langle S_i^A \rangle = \frac{\sum_i S_i^A e^{-\beta \mathcal{H}_A}}{\sum_i e^{-\beta \mathcal{H}_A}}, \qquad (4)$$

and substituting Eq. (3) into (4), yields

$$m_A = \frac{\sum_{i,j} S_i^A e^{-\beta\left[-J_1 \sum s_i^A s_j^B - D_A \sum s_i^{A^2}\right]}}{\sum_{i,j} e^{-\beta\left[-J_1 \sum s_i^A s_j^B - D_A \sum s_i^{A^2}\right]}}. \qquad (5)$$

Where S_i takes values (± 2, ± 1, 0) and assuming $\beta z_1 J_1 = t_1$, one obtains

$$m_A = \frac{2\, e^{2t_1 m_B + 4\beta D_A} - 2\, e^{-2t_1 m_B + 4\beta D_A} + e^{t_1 m_B + \beta D_A} - e^{-t_1 m_B + \beta D_A}}{e^{2t_1 m_B + 4\beta D_A} + e^{-2t_1 m_B + 4\beta D_A} + e^{t_1 m_B + \beta D_A} + e^{-t_1 m_B + \beta D_A} + 1}. \qquad (6)$$

By using the identities $e^x - e^{-x} = 2\sinh x$ and $e^x + e^{-x} = 2\cosh x$, Eq. (6) has the formula

$$m_A = \frac{2\sinh(2t_1 m_B) + e^{-3\beta D_A} * \sinh(t_1 m_B)}{\cosh(2t_1 m_B) + e^{-3\beta D_A} * \cosh(t_1 m_B) + \frac{1}{2} e^{-4\beta D_A}}, \qquad (7)$$

and,

$$\mathcal{H}_B = -J_1 \sum_{i,j} S_i^A S_j^B - J_2 \sum_{i,j} S_j^B S_j^B - D_B \sum_j \left(S_j^B\right)^2. \qquad (8)$$

So,

$$m_B = \langle S_j^B \rangle = \frac{\sum_j S_j^B e^{-\beta HB}}{\sum_j e^{-\beta HB}}. \qquad (9)$$

And substituting Eq. (8) into (9), it gives,

$$m_B = \frac{\sum_{i,j} S_j^B e^{-\beta\left[-J_1 \sum s_i^A s_j^B - J_2 \sum s_j^B s_j^B - D_B \sum s_j^{B^2}\right]}}{\sum_{i,j} e^{-\beta\left[-J_1 \sum s_i^A s_j^B - J_2 \sum s_j^B s_j^B - D_B \sum s_j^{B^2}\right]}}, \qquad (10)$$

where S_j takes values (± 7/2, ± 5/2, ±3/2, ±1/2) and assuming $\beta z_1 J_1 = t_1$ and $\beta z_2 J_2 = t_2$, the Eq (10) is written as

$$m_B = \frac{\frac{7}{2} e^{\frac{7}{2}t_1 m_A + \frac{7}{2}t_2 m_B + \frac{49}{4}\beta D_B} - \frac{7}{2} e^{-\frac{7}{2}t_1 m_A - \frac{7}{2}t_2 m_B + \frac{49}{4}\beta D_B} +}{e^{\frac{7}{2}t_1 m_A + \frac{7}{2}t_2 m_B + \frac{49}{4}\beta D_B} + e^{-\frac{7}{2}t_1 m_A - \frac{7}{2}t_2 m_B + \frac{49}{4}\beta D_B} +}$$

$$\frac{\frac{5}{2} e^{\frac{5}{2}t_1 m_A + \frac{5}{2}t_2 m_B + \frac{25}{4}\beta D_B} - \frac{5}{2} e^{-\frac{5}{2}t_1 m_A - \frac{5}{2}t_2 m_B + \frac{25}{4}\beta D_B} +}{e^{\frac{5}{2}t_1 m_A + \frac{5}{2}t_2 m_B + \frac{25}{4}\beta D_B} + e^{-\frac{5}{2}t_1 m_A - \frac{5}{2}t_2 m_B + \frac{25}{4}\beta D_B} +}$$

$$\frac{\frac{3}{2} e^{\frac{3}{2}t_1 m_A + \frac{3}{2}t_2 m_B + \frac{9}{4}\beta D_B} - \frac{3}{2} e^{-\frac{3}{2}t_1 m_A - \frac{3}{2}t_2 m_B + \frac{9}{4}\beta D_B} +}{e^{\frac{3}{2}t_1 m_A + \frac{3}{2}t_2 m_B + \frac{9}{4}\beta D_B} + + e^{-\frac{3}{2}t_1 m_A - \frac{3}{2}t_2 m_B + \frac{9}{4}\beta D_B} +}$$

$$\frac{\frac{1}{2} e^{\frac{1}{2}t_1 m_A + \frac{1}{2}t_2 m_B + \frac{1}{4}\beta D_B} - \frac{1}{2} e^{-\frac{1}{2}t_1 m_A - \frac{1}{2}t_2 m_B + \frac{1}{4}\beta D_B}}{e^{\frac{1}{2}t_1 mA + \frac{1}{2}t_2 mB + \frac{1}{4}\beta D_B} + e^{-\frac{1}{2}t_1 m_A - \frac{1}{2}t_2 m_B + \frac{1}{4}\beta D_B}}. \qquad (11)$$

Hence, Eq. (11) becomes

$$m_B = \frac{1}{2} \frac{7\sinh\left(\frac{7}{2}t_1 m_A + \frac{7}{2}t_2 m_B\right) + 5e^{-6\beta D_B} \sinh\left(\frac{5}{2}t_1 m_A + \frac{5}{2}t_2 m_B\right)}{\cosh\left(\frac{7}{2}t_1 m_A + \frac{7}{2}t_2 m_B\right) + e^{-6\beta D_B} \cosh\left(\frac{5}{2}t_1 m_A + \frac{5}{2}t_2 m_B\right)}$$

$$\frac{+3e^{-10\beta D_B} \sinh\left(\frac{3}{2}t_1 m_A + \frac{3}{2}t_2 m_B\right) + e^{-12\beta D_B} \sinh\left(\frac{1}{2}t_1 m_A + \frac{1}{2}t_2 m_B\right)}{+ e^{-12\beta D_B} \cosh\left(\frac{1}{2}t_1 m_A + \frac{1}{2}t_2 m_B\right) + e^{-10\beta D_B} \cosh\left(\frac{3}{2}t_1 m_A + \frac{3}{2}t_2 m_B\right)}. \qquad (12)$$

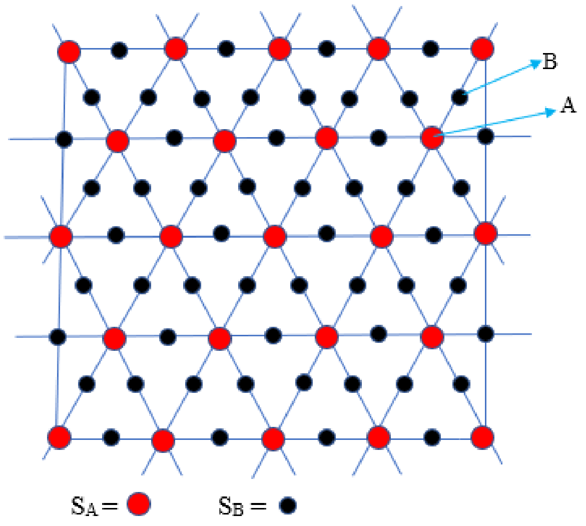

Fig. (1): Schematic representation of two-dimensionally ornamented triangular lattices. The red circles (A) indicate atoms with a spin of S_A=2, whereas the black circles (B) represent decorating atoms with a spin of S_B=7/2.

According to Equation (2), the system can achieve the most precise estimation of the current model by using a specified Hamiltonian. We employ a variational technique that calculates free energy based on the Bogoliubov inequality. By utilizing this approach, we can acquire the most precise estimation of the present model based on a particular Hamiltonian [12].

$$G \leq \Phi = G_o + \langle \mathcal{H} - \mathcal{H}_o \rangle_o . \tag{13}$$

Where G is the free energy of $\mathcal{H}$ given by (Eq 2), G_0 is the free energy of a trial Hamiltonian $\mathcal{H}_o$ depending on variational parameters, and $\langle ... \rangle o$ denotes a thermal average over the ensemble defined by $\mathcal{H}_o$. In this work, we consider one of the simplest possible choices of $\mathcal{H}_o$, namely,

$$\mathcal{H}_o = -\sum_i [\lambda_1 s_i^A + D_A (s_i^A)^2] - \sum_j [\lambda_2 s_j^B + D_B (s_j^B)^2]. \tag{14}$$

Where S_i^A takes the values of spins for nodal atoms and S_j^B with spin of atomic decorating. Whereas λ_1, λ_2, D_A and D_B are the variational parameters related to the different spins and the anisotropies of the two sublattices proposed (i.e., the nodal and decorating anisotropies), respectively. Researchers employ the partition function to articulate the connections between thermal properties, such as free energy and magnetization. The experimental Hamiltonian corresponds to the partition function [11], which is

$$Z_0 = \sum e^{-\beta \mathcal{H}_o} \tag{15}$$

Now, let us substitute Eq. (14) into Eq. (15) to obtain the partition function for the proposed model.

$$Z_0 = \sum_{\pm 2} e^{-\beta\{-\lambda_1 \Sigma S_i^A - D_A \Sigma\, S_i^{A^2}\}.-\lambda_2 \Sigma\, S_j^s - D_s \Sigma S_j^{s^2}\}} . \sum_{\pm\frac{7}{2}} e^{-\beta\{-\lambda_2 \Sigma\, S_j^B - D_B \Sigma S_j^{B^2}\}}. \tag{16}$$

$$Z_0 = \prod \{e^{2\beta\lambda_1 + 4\beta D_A} + e^{-2\beta\lambda_1 + 4\beta D_A} + e^{\beta\lambda_1 + \beta D_A} + e^{-\beta\lambda_1 + \beta D_A} + 1\}. \prod \{e^{\frac{7}{2}\beta\lambda_2 + \frac{49}{4}\beta D_B} + e^{-\frac{7}{2}\beta\lambda_2 + \frac{49}{4}\beta D_B} + e^{\frac{5}{2}\beta\lambda_2 + \frac{25}{4}\beta D_B} + e^{-\frac{5}{2}\beta\lambda_2 + \frac{25}{4}\beta D_B} + e^{\frac{3}{2}\beta\lambda_2 + \frac{9}{4}\beta D_B} + e^{-\frac{3}{2}\beta\lambda_2 + \frac{9}{4}\beta D_B} + e^{\frac{1}{2}\beta\lambda_2 + \frac{1}{4}\beta D_B} + e^{-\frac{1}{2}\beta\lambda_2 + \frac{1}{4}\beta D_B}\};$$

$$Z_0 = \{2e^{4\beta D_A}\cosh(2\beta\lambda_1) + 2e^{\beta D_A}\cosh(\beta\lambda_1) + 1\}^N . \left\{2e^{\frac{49}{4}\beta D_B}\cosh\left(\frac{7}{2}\beta\lambda_2\right) + 2e^{\frac{25}{4}\beta D_B}\cosh\left(\frac{5}{2}\beta\lambda_2\right) + 2e^{\frac{9}{4}\beta D_B}\cosh\left(\frac{3}{2}\beta\lambda_2\right) + 2e^{\frac{1}{4}\beta D_B}\cosh\left(\frac{1}{2}\beta\lambda_2\right)\right\}^{4N} . \tag{17}$$

It is possible to calculate the free energy by using the following Equation:

$$G_0 = -K_B T \ln Z_0 . \tag{18}$$

$$G_0 = -k_B TN \ln(2e^{4\beta D_A}\cosh(2\beta\lambda_1) + 2e^{\beta D_A}\cosh(\beta\lambda_1) + 1) - 4k_\beta TN \ln\left(2e^{\frac{49}{4}\beta D_B} cosh\left(\frac{7}{2}\beta\lambda_2\right) + 2e^{\frac{25}{4}\beta D_B} cosh\left(\frac{5}{2}\beta\lambda_2\right) + 2e^{\frac{9}{4}\beta D_B} cosh\left(\frac{3}{2}\beta\lambda_2\right) + 2e^{\frac{1}{4}\beta D_B} cosh\left(\frac{1}{2}\beta\lambda_2\right)\right). \tag{19}$$

Equation (13) is used to ensure precise findings. This Equation involves subtracting Eq. (14) from Eq. (2) to obtain the average value of the Hamiltonian.

$$\langle \mathcal{H} - \mathcal{H}_0 \rangle = \langle -J_1 \Sigma\ S_i^A S_j^B - J_2 \Sigma\ S_j^B S_j^B - D_A \Sigma A_i^{A^2} - D_B \Sigma\ S_i^{B^2} + \lambda_1 \Sigma\ S_i^A + \lambda_2 \Sigma\ S_j^B + D_A \Sigma\ S_i^{A^2} + D_B \Sigma\ S_j^{B^2} \rangle.$$

Where $\beta = \frac{1}{k_B T}$; $< S_i^A S_j^B > = m_A m_B$; $< \Sigma\ S_i^A S_j^B > = z m_A m_B$; $m_A =< S_i^A >$;

$m_B =< S_i^B >$, note that m_A and m_B represent the magnetization of sublattices A and B, respectively.

$$\langle \mathcal{H} - \mathcal{H}_0 \rangle = -J_1 N Z_1 m_A m_B - 4NJ_2 Z_1 m_B^2 + \lambda_1 N m_A + 4N\lambda_2 m_B . \tag{20}$$

Now, by substituting equations (19) and (20) into Equation (13), we get the free energy of the model in question from the formula:

$$\frac{G}{N} = g = -k_B T \left\{\ln\left(2e^{4\beta D_A}\cosh(2\beta\lambda_1) + 2e^{\beta D_A}\cosh(\beta\lambda_1) + 1\right) + 4\ln\left(2e^{\frac{49}{4}\beta D_B}\cosh\left(\frac{7}{2}\beta\lambda_2\right) + 2e^{\frac{25}{4}\beta D_B}\cosh\left(\frac{5}{2}\beta\lambda_2\right) + 2e^{\frac{9}{4}\beta D_B}\cosh\left(\frac{3}{2}\beta\lambda_2\right) + 2e^{\frac{1}{4}\beta D_B}\cosh\left(\frac{1}{2}\beta\lambda_2\right)\right)\right\}$$

$$-J_1Z_1m_Am_B - 4J_2Z_1m_B^2 + \lambda_1 m_A + 4\lambda_2 m_B . \qquad (21)$$

To calculate the value of λ_1, we use the following relationship:

$$\frac{\partial g}{\partial \lambda_1} = 0,$$

$$\frac{\partial g}{\partial \lambda_1} = -k_\beta T\left\{\frac{2e^{4\beta D_A}\sinh(2\beta\lambda_1)\cdot 4\beta + e^{\beta D_A}\sinh(\beta\lambda_1)\cdot 2\beta}{2e^{4\beta DA}\cosh(2\beta\lambda_1) + 2e^{\beta D_A}\cosh(\beta\lambda_1) + 1}\right\} - J_1Z_1m_B\frac{\partial mA}{\partial \lambda_1} + \lambda_1\frac{\partial mA}{\partial \lambda_1} + m_A = 0 ,$$

$$-m_A + m_A + (\lambda_1 - J_1 z_1 m\beta)\frac{\partial m_A}{\partial \lambda_1} = 0 ,$$

$$\lambda_1 = J_1Z_1m_B . \qquad (22)$$

And to calculate the value of λ_2, one has,

$$\frac{\partial g}{\partial \lambda_2} = 0 ,$$

$$\frac{\partial g}{\partial \lambda_2} = -4k_\beta T\left\{\frac{1}{2}\,\frac{2e^{\frac{49}{4}\beta D_B}\sinh\left(\frac{7}{2}\beta\lambda_2\right)\cdot\frac{7}{2}\beta + 2e^{\frac{25}{4}\beta D_B}\sinh\left(\frac{5}{2}\beta\lambda_2\right)\cdot\frac{5}{2}\beta + 2e^{\frac{9}{4}\beta D_B}\sinh\left(\frac{3}{2}\beta\lambda_2\right)\cdot\frac{3}{2}\beta + 2e^{\frac{1}{4}\beta D_B}\sinh\left(\frac{1}{2}\beta\lambda_2\right)\cdot\frac{1}{2}\beta}{e^{\frac{49}{4}\beta DB}\cosh\left(\frac{7}{2}\beta\lambda_2\right) + e^{\frac{25}{4}\beta D_B}\cosh\left(\frac{5}{2}\beta\lambda_2\right) + e^{\frac{9}{4}\beta D_B}\cosh\left(\frac{3}{2}\beta\lambda_2\right) + e^{\frac{1}{4}\beta DB}\cosh\left(\frac{1}{2}\beta\lambda_2\right)}\right\} -$$

$$J_1Z_1m_A\frac{\partial m_B}{\partial \lambda_2} - 8J_2Z_1m_B\frac{\partial m_B}{\partial \lambda_2} + 4\lambda_2\frac{\partial m_B}{\partial \lambda_2} + 4m_B = 0 ,$$

$$-4m_B + 4m_B + (4\lambda_2 - 8J_2Z_1m_B - J_1Z_1m_A)\frac{\partial m_B}{\partial \lambda_2} = 0,$$

$$\lambda_2 = 2J_2z_1m_B + \frac{J_1}{4}z_1m_B . \qquad (23)$$

Now, by substituting equations (22) and (23) into Equation (21), we get the free energy of the model as in,

$$g = -k_B T\left\{\ln\left(2e^{4\beta D_A}\cosh(2\beta J_1Z_1m_B) + 2e^{\beta D_A}\cosh(\beta J_1Z_1m_B) + 1\right\} - 4k_\beta T\left\{\ln\left(2e^{\frac{49}{4}\beta D_B}\cosh\left(7\beta J_2Z_1m_B + \frac{7}{8}\beta J_1Z_1m_A\right) + 2e^{\frac{25}{4}\beta D_B}\cosh\left(5\beta J_2Z_1m_B + \frac{5}{8}\beta J_1Z_1m_A\right) + 2e^{\frac{9}{4}\beta D_B}\cosh\left(3\beta J_2Z_1m_B + \frac{3}{8}\beta J_1Z_1mA\right) + 2e^{\frac{1}{4}\beta D_B}\cosh\left(\beta J_2Z_1m_B + \frac{1}{8}\beta J_1Z_1m_A\right)\right)\right\} + 4J_2Z_1m_B^2 + J_1Z_1m_Am_B . \qquad (24)$$

Notably, in the case of ferrimagnetic materials, distinct indications of sublattice magnetizations are observed, and a point of compensation exists where the total longitudinal magnetization is precisely zero. The aggregate magnetization of the Ising model on a two-dimensional decorated triangular lattice (z=6; z is the number of nearest neighbours of the sublattice) is [13,14],

$$M = \frac{m_A + \frac{z}{2}m_B}{4} = \frac{m_A + 3m_B}{4} . \qquad (25)$$

III. Results and discussion

By altering the crystal field parameters, we examined the relationship between the temperature variation and the sublattice magnetizations of a triangular Blume Capel system with a mixture of spin-2 and spin-7/2, as shown in Figs. 2 and 3. The ornamented ferrimagnetic model, which was numerically examined, revealed typical behaviours inside the mean field approximation (MFA). We implement the strategy by utilizing the minimizing free energy function described in Equation (24). The primary method entails studying the phenomenon of superparamagnetism in a decorated ferrimagnetic mixed triangular system. We investigated the impact of the recommended alloy's low temperature on the curves of magnetization and magnetic anisotropies. This study analyzes a particular case within a decorated ferrimagnetic mixed spin triangle system's (m_A, T) and (m_B, T) planes. We have examined the impact of altering the spin crystal fields $D_B/|J_2|$ and $D_A/|J_2|$ on the system, as seen in Figs. 2 and 3, respectively. More precisely, when the values of decorated atoms $D_A/|J_2|$=-0.5, J_1=-0.5, and J_2=-1 are kept constant, the sublattices display different magnetization patterns within the range of (-4.5 $\leqslant D_B/|J_2| <$ 2.5), as seen in Fig. 2. It is essential to highlight that sublattice magnetization undergoes a first-order phase transition, achieving zero or a different value [14, 25]. The sublattice magnetization can quickly altered that it does go to zero when the system transitions between two phases, separating the ferrimagnetic or antiferromagnetic phase from the paramagnetic phase. According to Figure 3, at a temperature of 0 Kelvin, the magnetizations of sublattices m_A and m_B are influenced by the decorated crystal field $D_A/|J_2|$, with mA starting from minimal values of -2, -1.5, and -1, while m_B starts from its maximum value of 3.5. The magnetizations are highly influenced by the positive and negative values of $D_A/|J_2|$ as the temperature rises. Specifically, when $D_A/|J_2|$ takes on values of 2.5, 1.5, 0.5, -0.5, -1.5, and -2.5, the magnetizations consistently approach zero. Given that D_A/|J2|=-3.5,-4.5, and J_1= -0.5, J_2=-1, it can be shown that it occurs at a temperature where the magnetizations undergo a discontinuous change. A first-order transition occurs when the magnetization undergoes a sudden change, resulting in the emergence of new phases at (-1.5, 0.5) and (-1, 3.5) for $D_B/|J_2|$=-4.5 and $D_A/|J_2|$=-4.5, respectively. Similarly, for $D_A/|J_2|$=-0.5 and $D_B/|J_2|$=0.5, the transition is illustrated in Figs. 2 and 3.

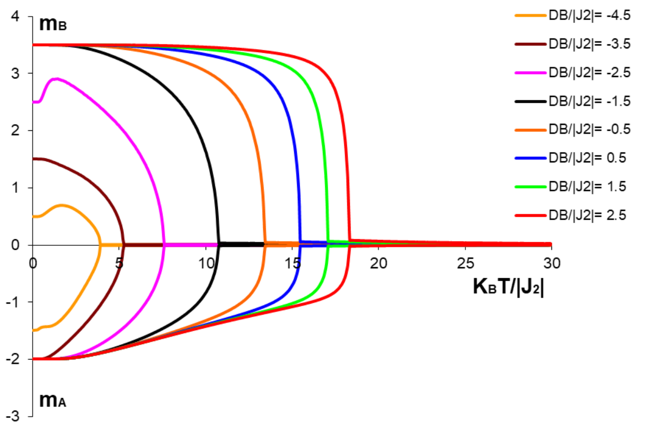

Fig. 2 The sublattice magnetizations of a decorated ferrimagnetic mixed-spin triangular system are dependent on the temperature at various values of $D_B/|J_2|$, with a constant value of $D_A/|J_2|$=-0.5 and J_1=-0.5 and J_2=-1.

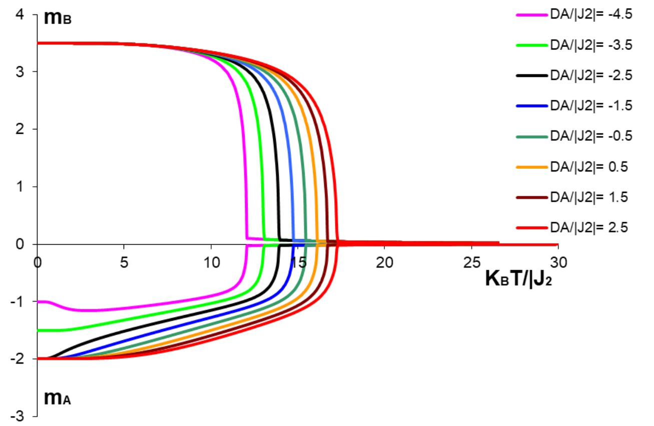

Fig. 3 Variation of sublattices magnetizations with temperature for a decorative ferrimagnetic mixed-spin triangle system with a fixed value of $D_B/|J_2|$=0.5, J_1=-0.5, and J_2=-1.

Let us examine Fig. 4, which displays the overall magnetization as a function of the absolute temperature. It shows us significant results that indicate the occurrence of a vital magnetism phenomenon: the compensation temperature. When the system is exposed to changes in the magnetic anisotropy of the sublattices of atom B while keeping the magnetic anisotropy of atom A constant, this phenomenon occurs at absolute zero. We use a decorated triangular lattice (z = 6), where (D_A /$|J_1|$ = 1), with, J_1 = -1, J_2 = -0.5, and when increasing temperature and before reaching the paramagnetic phase, the magnetic spins are in the ferromagnetic state. At values of D_B /$|J_1|$ =-2, -2.5, -3, with a fixed value of (D_A /$|J_1|$ = 1), the system has one compensation temperature for each value. As the temperature affecting the system increases, it becomes in the paramagnetic phase. The material does not undergo the compensation phenomenon at (D_B /$|J_1|$ = -0.5, -1, -1.5). It is worth noting that these results confirm that the anisotropy of crystalline magnetism plays an essential role in limiting the compensation phenomenon and determining the location of the compensation temperatures. We differ in this interpretation with the results of research [19], which confirm that anisotropy exclusively affects the position of the compensation temperature. At the same time, we agree with the research results [20] that crystalline anisotropy affects the results and appearance of the compensation temperatures; moreover, the results we obtained are distinctive and encouraging and agree with the researchers' results. [21, 22], respectively. The phenomenon of compensation occurs due to entropy, which refers to the measure of irregularity in the magnetic lattice, as it is observed that the colonies of magnetic spins align with each other in the crystal lattice for the magnetic spins mA, and to an extent more significant than the alignment of the magnetic spins of the sublattices of atoms B, when the temperature increases, affecting the system as a whole. By changing the magnetic anisotropies alike, the opposite occurs until at a specific value of the magnetic contrasts, it becomes m_A=-m_B, and the total spin magnetic system under study is zero, but it is in the ferromagnetic phase. At this temperature, the phenomenon of compensation occurs. As the temperature increases, the system enters the paramagnetic phase and eventually loses magnetism completely. Figure 5 illustrates a single compensation temperature for various $D_A/|J_1|$ values while keeping $D_B/|J_1|$ constant. This observation aligns with the Neel hypothesis, categorizing it as an N-type behaviour [20]. On the other hand, the magnetic characteristics of the suggested system have been investigated for various values of $D_A/|J_1|$, with a fixed value of $D_B/|J_1|$=-3. Nevertheless, the magnetization curves steadily decline, distinguishing the ferrimagnetic phase from the paramagnetic phase. The occurrence is called a second-order phase transition or the Curie temperature [13,24, 25].

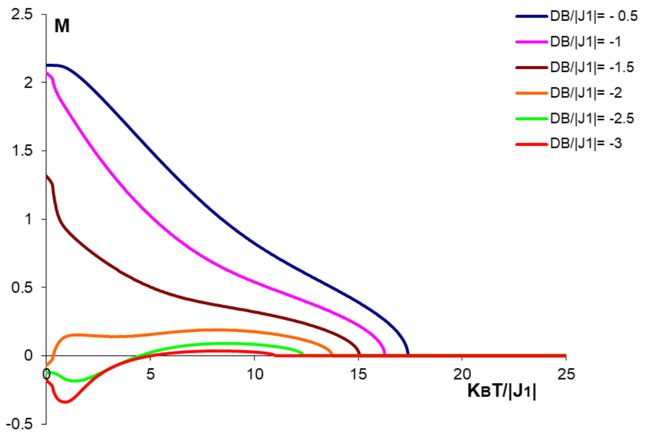

Fig.4 The temperature effects on the total magnetizations M of an ornamented ferrimagnetic mixed spin triangular system at various $D_B/|J_1|$ values, with $D_A/|J_1|$ = 1 and J_1 = -1 and J_2 = -0.5.

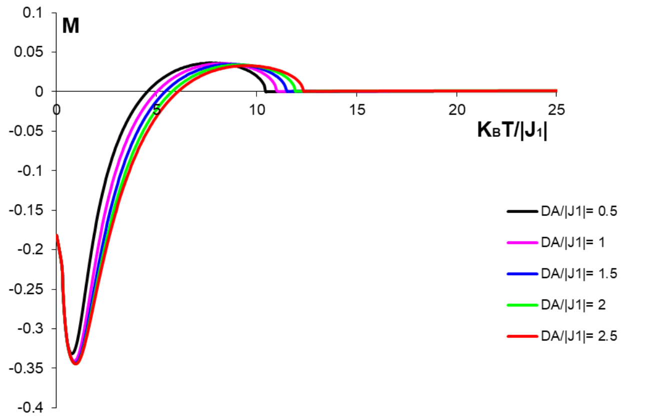

Fig. 5 The total magnetizations M of a decorated ferrimagnetic mixed spin triangular system depend on the temperature at various $D_A/|J_1|$ values, with $D_B/|J_1|$ holding constant at -3, J_1 = -1, and J_2 = -0.5.

Now, let us examine Fig (6), which displays the overall magnetization as a function of the absolute temperature and presents necessary behaviour experienced by the magnetic system under study when an external magnetic field is applied with a range of ($0 \leqslant H/|J_2| \leqslant 0.5$) when ($D_A/|J_1|$ = 0.5) and ($D_B/|J_1|$ = -3.5) with values of J_1 = -1 and J_2 = -0.5 for a decorated triangular lattice. The system shows distinct behaviour: one compensation point for each $H/|J_1|$ value. It is worth noting that these results are important and worthy of study because they give the impression that the system, under specific conditions of crystal anisotropy, possesses alternating magnetism.

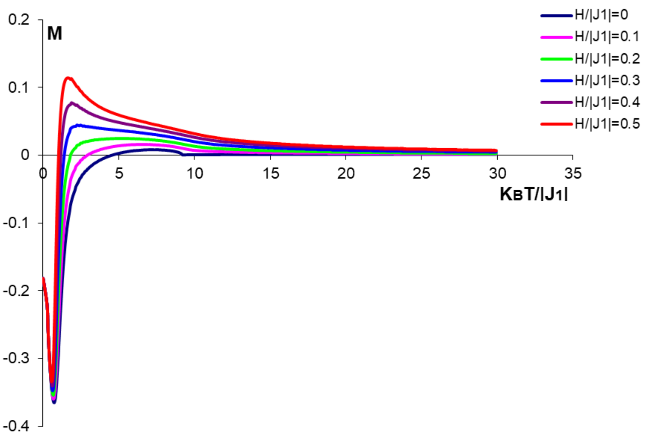

Fig. 6: The temperature dependences of the total magnetizations M of a decorated ferrimagnetic mixed-spin triangular system for various values of $H/|J_2|$, with $D_A/|J_2|$ = 0.5, $D_B/|J_2|$ = -3.5, and J_1 = -1 and J_2 = -0.5.

At a fixed value of $D_B/|J_2|$ = -0.5, where $J_1 = -0.5$ and $J_2 = -1.0$, Fig. (7) shows how the residual magnetization of the total magnetization changes when the magnetic anisotropy of a decorated triangular lattice, specifically a nodular sublattice, is changed. The overall magnetization diminishes with an increase in the absolute value of $D_A/|J_2|$.Specifically, when $D_A|J_2| > 0$, this reduction influences the variation of the total magnetization in the context of a decorated ferrimagnet under consideration. The residual magnetization is the term used to describe the condition of a decorated ferrimagnet that is magnetized without any external influence, indicating that its magnetization is not zero ($M \neq 0$) [23, 24]

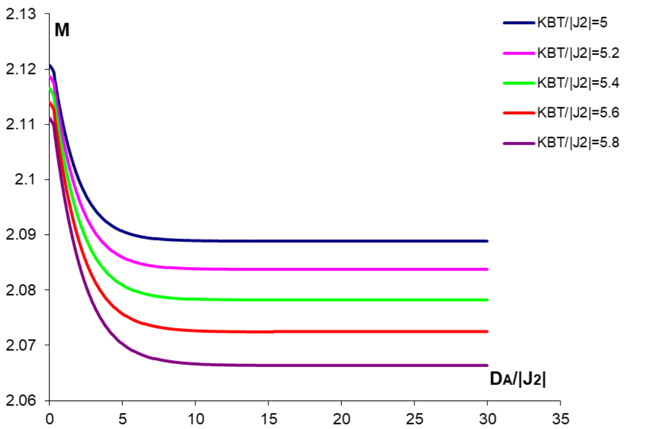

Fig.7. The relationship between the crystal field $D_A/|J_2|$ and the global magnetization M for a decorated ferrimagnetic mixed spin triangular system. $D_B/|J_2|$ = -2.5, with J_1 = -0.5 and J_2 = -1.0.

Conversely, Fig. 8 demonstrates that as the ratio $D_B/|J_2|$ grows, the total magnetization undergoes a modest shift initially and then increases when $D_B/|J_2| > 0$. The magnetization rapidly increases until it reaches a saturation point, considerably influenced by the absolute temperature. The authors [6] employed Monte Carlo computations to investigate the magnetic properties of decorated ferrimagnetic mixed spin-3/2 and spin-5/2 Ising systems, juxtaposing our findings. Furthermore, it is worth noting that our present system demonstrates superparamagnetic characteristics when the crystal field $D_B/|J_2|$ = 0, which leads to an overall magnetization of zero [9]. Our decorated system generates superparamagnetic phenomena at $D_A/|J_2|$ = -2.5, where $J_1 = -0.5$ and $J_2 = -1$, as shown in Fig. 8. The observed results closely align with the conclusions drawn by A. Jabar and R. Masrour [9]. Researchers found that increasing the crystal field leads to a rise in overall magnetization for various exchange interaction configurations involving decorating ions within a square lattice and between nodal and decorating ions. The relationship between the external magnetic field H/J_2 and the total magnetization M is illustrated in Fig. 9. The system is a decorated ferrimagnetic mixed spin triangular system with fixed values of $D_A/|J_2|$=8 and $D_B/|J_2|$=-11. For ($K_BT/|J_2|$ = 2,2.5,3,3.5,4) K^o, J_1 = -0.5 and J_2 = 1, respectively. As the magnitude of $H/|J_2|$ grows, the total magnetization initially undergoes modest variations and eventually increases when $H/|J_2| > 0$. The magnetization rapidly increases until it reaches a saturation point, considerably influenced by the absolute temperature. In addition, our current system exhibits superparamagnetic behaviour when the external magnetic field $H/|J_2|$ = 0, resulting in a total magnetization of zero.

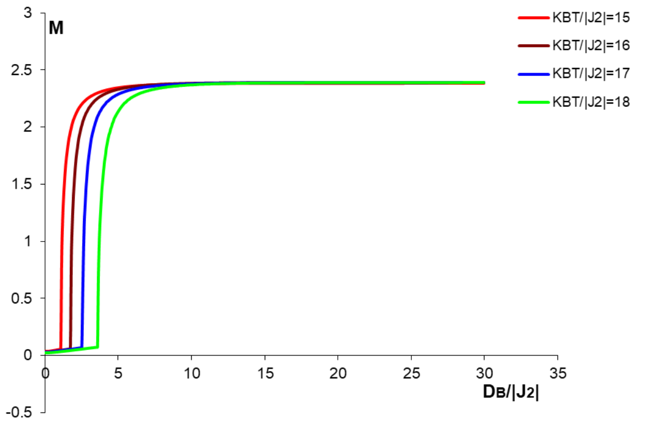

Fig.8 The crystal field dependences $D_B/|J_2|$ of the total magnetization M for a decorated ferrimagnetic mixed spin triangular system, with a constant value of $D_A/|J_2|$=-2.5, with J_1 = -0.5, J_2 = -1.0.

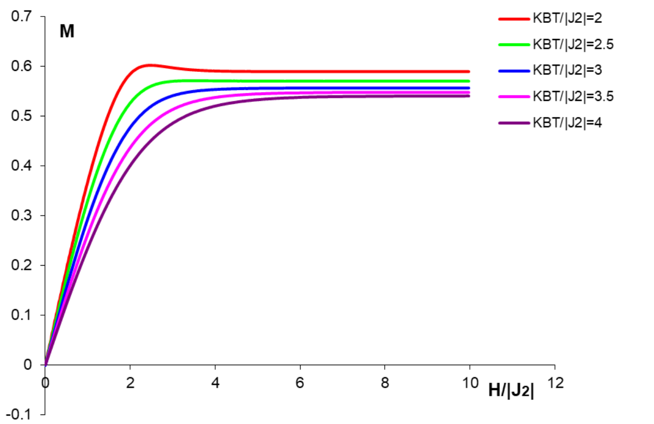

Fig.9 The magnetic field $H/|J_2|$ of the total magnetization M for a decorated ferrimagnetic mixed spin triangular system, with fixed values of $D_A/|J_2|$=8. and $D_B/|J_2|$=-11, with J_1 = -0.5, J_2 = 1

IV. Conclusions

We employed the mean field technique to clearly study the magnetic properties of a decorated ferrimagnetic mixed-spin (2,7/2) triangular Blume-Capel device. The investigation centers on the influence of crystal fields and external magnetic fields on magnetization phenomena. The ferrimagnetic crystal domains have been carefully changed that one may reveal interesting phenomena are the behaviors of compensation, reentrance, and superparamagnetism, respectively. Figure 8 demonstrates that our current system displays superparamagnetic characteristics within the 15K^o ⩽ $K_BT/|J_2|$ ⩽ 18 K^o range. This complex ferrimagnetic mixed spin triangular system has a constant ratio of $D_A/|J_2|$ = -2.5, J_1 = -0.5, and J_2 = -1.0. Supermagnetism is shown in Fig. (9) by examining the correlation between the overall magnetization and the external magnetic field. This analysis is conducted on a decorated ferrimagnetic mixed spin triangular system, with a constant value of D_A / $|J_2|$=8 and D_B / $|J_2|$=-11, while J_1 = -0.5 and J_2 = 1, respectively. One compensation temperature is induced as shown in Fig.4, for each value of decorated magnetic anisotropy (0.5 ⩽ $D_A/|J_1|$⩽2.5) while maintaining a fixed value of $D_B/|J_1|$=-3, where J_1 =-1 and J_2 =-0.5. In addition, one compensation temperature for various values of decorated magnetic anisotropy is illustrated in Fig. 5, where $D_B/|J_1|$⩽-3 and $D_A/|J_1|$=1, with J_1 = -1 and J_2 = -0.5, are held constant. Figure 6 illustrates the compensation temperature associated with each value for which the external magnetic field varies: 0 ⩽ $H/|J_1|$⩽ 0.5, $D_A/|J_1|$=0.5, $D_B/|J_1|$=-3.5, J_1 = -1, J_2 = -0.5. However, we can still compare our findings to the results of M. Boughrara and M. Kerouad in their study on the decorated Ising film with a cubic lattice layout. The system consists of (1/2,1) ions, and Monte Carlo simulation indicates the presence of one or two compensatory temperatures [5]. At a constant value of D_B / $|J_2|$ = -2.5, with J_1 = −0.5 and J_2 = −1.0, and for $K_BT/|J_2|$ = 5, 5.2, 5.4, 5.6, and 5.8K^o, respectively, the picture in Fig. 7 shows how the overall magnetization is related to the magnetic anisotropy of a decorated sublattice, also known as a nodal sublattice. D_A / $|J_2|$ represents the magnetic anisotropy. The total magnetization decreases as the magnitude of D_A / $|J_2|$ increases. Specifically, when $D_A/ |J_2| > 0$, this decrease affects the variation of the total magnetization in the considered decorated ferrimagnet. Residual magnetization occurs when a decorated ferrimagnet becomes magnetized without external influence, resulting in a non-zero magnetization value (M ≠ 0). [23, 24].

CONFLICT OF INTEREST

Authors declare that they have no conflict of interest.

REFERENCES

[1]. S. Bedanta, W. Kleemann. "Supermagnetism" *J. Phys. D Appl. Phys.* 42 (2009), 013001, https://doi.org/10.1088/0022-3727/42/1/013001.

[2]. O. Raita, et al. "Superparamagnetic behavior of ZnFe204 nanoparticles as evidenced by EPR." *J. Optoelectron. Adv. Mater* 17.9-10,2015.

[3]. Y. Nakamura, "Monte Carlo simulation of mixed S = 2 and S = 5/2 Ising system," Prog. *Theor. Phys. Suppl*, no. 138, pp.466-467,2000, doi:10.1143/PTPS.138.466.

[4]. V. Stubňa and M. Jaščur, "Mixed spin-1/2 and 3/2 Ising model with multipin interactions on a decorated square lattice," *J. Magn. Magn. Mater*, vol 442, pp364-370, 2017, doi:10. 1016/j. jmmm. 2017.07. 011.

[5]. M. Boughrara and M. Kerouad, "Phase transition and magnetic properties of a decorated Ising film: Monte Carlo and effective field treatments". *Phys. A* Stat.387, no.24, PP.6105-6114, 2008, doi: 10.1016/j.physa.2008.07.006.

[6]. R. Masrour, A. Jabar, A. Benyoussef, and M. Hamedoun, "Comparable studies of magnetic properties of Ising spins-5/2 and 3/2 systems on decorated square and triangular lattices", *J. Magn. Magn. Mater.*, vol. 410, pp. 223-225, 2016, doi: 10.1016/j.jmmm.2016.03.035.

[7]. M. Karimou and N. De La Espriella, "Critical phenomena in a two-dimensional ferrimagnetic system: Monte Carlo and Mean-Field Analysis," *Phys. A Stat. Mech. its Appl.*, vol. 531, p. 121738, 2019, doi: 10.1016/j.physa 2019.121738.

[8]. H K. Mohamad, "Crystal fields induced compensation temperatures in a decorated square lattice," *Indian J. Phys*., 2022, doi: 10.1007/s12648-022-02280-9.
[9]. A. Jabar and R. Masrour, "Magnetic properties of mixed spin-5/2 and spin-2 Ising model on a decorated square lattice: A Monte Carlo simulation," *Phys. A Stat. Mech. its Appl.,* vol. 515, pp.270-278,2019,doi: 10.1016/j.physa.2018.09.190.
[10]. H. Jie Song, S. You, X. Hualia, J. Yang. "MoS2 nanosheets decorated with magnetic Fe3O4 nanoparticles and their ultrafast adsorption for wastewater treatment" V. 41, Issue 10, P. A, December 2015, PP. 13896-13902.
[11]. J.M. Yeomans, Statistical Mechanics of Phase Transitions, Oxford University Press,1992.
[12]. B. Deviren, M. Keshin, "Dynamic Phase Transitions and Compensation Temperatures in a Mixed Spin-3/2 and Spin-5/2 Ising System", *J State Phys*, Vol. 140, pp.934-947, 2010.
[13]. W. Wang, et al. "Effects of the single-ion anisotropy on magnetic and thermodynamic properties of a ferrimagnetic mixed-spin (1, 3/2) cylindrical Ising nanowire." *Super lattices and Microstructures* 98,2016.
[14]. A. Feraoun, M. Kerouad, the mixed spin-(1,3/2) Ising nanowire with core/inter shell/outer-shell morphology, *Appl. Phys*. A, 2018.
[15]. T. Kaneyoshi, M. Jascur and Tomczak, "The Ferrimagnetic Mixed Spin-1/2 and -3/2 Ising system", *J. Phys*.: Condens. Matter 4, pp. L653- L658, 1992.
[16]. A. Bobak and M. Jascur, "Correlated Effective-Field Theory of the Site-Diluted Ising Model," *Journal of Magnetism and Magnetic Materials* 136, pp. 105-117, 1994.
[17]. H. K. Mohamad, "Magnetic and Thermodynamic Properties of a Mixed Spin-1 and Spin -7/2 Blume-Capel Ising Ferrimagnetic System", *International Journal of Advanced Research*, Vol. 2, No. 9, pp. 442-453, 2014.
[18]. F. Abubrig, "Mean-Field Solution of The Mixed Spin-2 and Spin-5/2 Ising Ferrimagnetic System with Different Single-Ion Anisotropies", *Open Journal of Applied Sciences*, pp. 270-277, 2013.
[19]. A. Dakhama, N. Benayad "On the existence of compensation temperature in 2d mixed-spin Ising ferrimagnetic: an exactly solvable model", *J. Magn. Magn. Mater*,213,2000,117.
[20]. A. Bobak, "The Effect of Anisotropies on The Magnetic Properties of a Mixed Spin-1 and Spin-3/2 Ising Ferrimagnetic System", *Physica A* 258, pp. 140-156, 1998.
[21]. J. Oitmaa and I. G. Enting, "A series of a Mixed-Spin *S* = (1/ 2,1) Ferrimagnetic Ising Model", *J. Physica Condens. Matter*, Vol. 18, pp. 10931-10942, 2006.
[22]. B. Deviren, M. Keskin, and O. Canko, "Magnetic Properties of an Antiferromagnetic and Ferrimagnetic Mixed Spin-1\2 and Spin-5\2 Ising Model in The Longitudinal Magnetic Field within The Effective-Field Approximation", *Physica A* 388, PP. 1835-1848, 2009.
[23]. H. Miao, G. Wei, J. Geng, Phase transitions and I multicritical points in the mixed spin-3/2 and spin-2 Ising model with different single-ion-anisotropies, *J. Magn. Magn. Mater.*, vol.321, p.4139(2009).
[24]. B. Boughazi, M Boughrara, M Kerouad, Phase diagrams and magnetic properties of ferrimagnetic mixed spin- 1/2and spin-3/2 Ising nanowire, *Physica A*.vol.465, p. 628(2017).
[25]. M. Boughrara, M. Kerouad, and M. Saber, "Effect of a random longitudinal field and crystal field on a decorated ferrimagnetic Ising model," *J. Magn. Magn. Mater.*, vol. 316, no.2 SPEC. ISS., pp. 287-290, 2007, doi:10.1016 j. jmmm.2007.02.120.